



Rheological properties of cemented gangue backfill material based on fractal characteristics of waste coal gangue

Xiaoli Ye^{1,2} · Yuxia Guo^{1,2} · Guorui Feng^{1,2,3,4} · Xiaoxuan Wang^{1,2} · Weiyang Hu^{1,2} · Jiahui Ma^{1,2}

Received: 12 October 2022 / Accepted: 17 January 2023 / Published online: 9 February 2023
© The Author(s), under exclusive licence to Springer-Verlag GmbH Germany, part of Springer Nature 2023

Abstract

The study herein was intended to evaluate the rheological properties of cemented gangue backfill material (CGBM). For this purpose, the rheological test of CGBM with fractal aggregate particle size distribution was carried out, and variations of static yield stress, dynamic yield stress, and plastic viscosity were investigated as a function of fractal dimension and time. The results reveal that aggregate particle size distribution exerts a significant influence upon the rheological properties of CGBM, and with the escalation of the fractal dimension of the aggregate, the yield stress and plastic viscosity initially decline and then increase. In addition, with elapsing time, the correlation between the static yield stress and the fractal dimension of CGBM specimens increases, while the correlations between the dynamic yield stress and the plastic viscosity and the fractal dimension decrease. The relationships between rheological parameters and fractal dimensions at different times are established based on the experimental results. The influence mechanism of aggregate particle size distribution on CGBM is analyzed from the perspective of the aggregate packing state. This study can provide a basis for the ratio design of CGBM in backfill mining.

Keywords Rheological properties · Coal gangue · Fractal dimension · Yield stress · Plastic viscosity · Compressible packing model (CPM)

Introduction

Backfill mining is an important element of the coal mine green mining system, which can effectively control ground pressure and reduce the massive accumulation of waste coal gangue, thereby protecting the safety of coal miners and achieving sustainable development of the ecological environment (Deng et al. 2017; Wang et al. 2022; Yilmaz et al.

2014; Feng et al. 2022; Ran et al. 2022; Zhao et al. 2022a, b; Xue et al. 2021). The cemented gangue backfill material (CGBM) used for backfill mining is mainly composed of cementitious materials, fly ash, coal gangue, and water, and transported to the goaf through pipelines for filling (Guo et al. 2020; Sun et al. 2019; Wu et al. 2015). The rheological characteristics of the CGBM mixture in the pipeline will affect the transportation efficiency and filling effect directly (Wang et al. 2020; Zhang et al. 2008; Chen et al. 2022a, b). Therefore, to ensure the security and efficient transportation of CGBM mixture and excellent filling quality, it is necessary to study the rheological characteristics of CGBM. Furthermore, the rheological characteristics of CGBM are mainly related to its material composition (Qi et al. 2015), of which gangue aggregate in the CGBM accounts for the largest proportion, oftentimes can generally reach 50~80%. Aggregate particle size distribution has a great impact on the interaction force between aggregates and the flow resistance caused by aggregates in the CGBM mixture (Wu et al. 2021a, b). Therefore, it is of great significance to investigate the influence of aggregate particle size distribution on the rheological properties of CGBM.

Responsible Editor: Philippe Garrigues

✉ Yuxia Guo
gyx771221@163.com

- ¹ College of Mining Engineering, Taiyuan University of Technology, Taiyuan 030024, Shanxi, China
- ² Shanxi Province Research Centre of Green Mining Engineering Technology, Taiyuan, Shanxi, China
- ³ Shanxi Province Coal-Based Resources Green and High-Efficiency Development Engineering Center, Taiyuan, Shanxi, China
- ⁴ Shanxi-Zheda Institute of Advanced Materials and Chemical Engineering, Taiyuan, Shanxi, China

Currently, a lot of research has been conducted on the effect of aggregate particle size distribution on the rheological properties of slurry. (Gao et al. 2022; Mahaut et al. 2008; Li et al. 2021). Yan et al. (2020) adopted a random aggregate generation algorithm to simulate the aggregate gradation and revealed that the coarse aggregate settles easily in the mortar when the coarse aggregate content is high and the mortar yield stress is low, thus leading to self-compacting concrete segregation. Feng et al. (2016) examined the influence of the mixed aggregate ratio of gangue and waste concrete on the rheological properties of the CGBM mixture and concluded that the CGBM has good flowability when the fine aggregate replacement rate of waste concrete is 37% and the coarse aggregate replacement rate of waste concrete is 49%. Gismera et al (2020) studied the effect of aggregates with different particle size distributions on the rheological properties of alkaline mortar and found that the plastic viscosity of the mortar is closely related to the packing density and void ratio of the aggregates. Liu et al. (2016) used Fuller's grading theory to optimize the gradation of mixed aggregates of all-tailed sand and water-hardened slag, and found that the mixed aggregate system had a larger stacking density and a lower pipe flow resistance of the paste when the grading index was 0.3. Hu and Wang (2011) investigated the effect of different graded aggregate grades on the rheological properties of concrete and found that the higher the content of coarse and fine aggregates, the higher the concrete rheological parameters (plastic viscosity and yield stress), and for a certain volume of mortar, yield stress and viscosity typically increase with the content of uncompressed voids and friction angle, while decreasing with the size of coarse aggregates.

Some scholars have employed fractal theory to describe particle distribution characteristics quantitatively. Wu et al. (2021a, b) investigated the effect of aggregate particle size distribution on the mechanical properties of the backfill in accordance with fractal theory, and found that the ultrasonic velocity and compressive strength of the backfill had a quadratic polynomial relationship with the fractal dimension of the aggregate particle size distribution. Chen et al. (2022a, b) analyzed the relationship between the fractal dimension of fibrous concrete crushed particles and fracture energy based on fractal theory and concluded that the dynamic compressive strength and fracture energy of fibrous concrete increase with the increase of fractal dimension at different strain rates. Liang et al. (2020) examined the fractal dimension characteristics of concrete fragments applying fractal theory and established the relationship between energy consumption density and fractal dimension, and revealed that the fragmentation severity and fractal dimension of debris increased with the increase of impact speed under the same fiber content. Ren and Xu (2016) investigated the fractal characteristics of

concrete debris produced by impact crushing and realized that the corresponding fractal dimension calculated by the mass-size relationship is an ideal indicator to describe the degree of debris. Li et al. (2019) investigated the fractal dimensional characteristics of concrete fractions subjected to impact by freeze–thaw cycles, established the relationship between energy consumption density and fractal dimension of fragments, and revealed the coupling effect of freeze–thaw cycles and strain rate on fractal characteristics and energy consumption.

It can be seen that the above studies use the fractal dimension to characterize the particle size distribution of aggregates. However, most of the researches focus on the mechanical properties of the materials, and there are few studies on the rheology of the materials. Although the time-dependent change of the rheological properties of concrete has been studied, the rheological properties of CGBM have been examined less. On this basis, this paper will explore the fractal characteristics of aggregate gradation and establish the connection between the fractal dimension of aggregate gradation and rheological parameters. The correlations between aggregate gradation and rheological parameters are analyzed with time variation. And the compressible packing model (CPM) is also used to reveal the influence mechanism of aggregate particle size distribution on the rheology of the CGBM mixture. This study can provide a reference for optimizing the particle size distribution of the aggregates of CGBM.

Experimental methods

Raw materials

The CGBM is composed of cement, fly ash, coal gangue, and water according to the mass ratio of 1:2:5:2 evenly mixed (Guo et al. 2022; Zhao et al. 2022a, b; Du et al. 2019). The cement is ordinary Portland cement 42.5 produced by Taiyuan Shishou Cement Co., with a specific surface area of 4500cm²/g, and initial and final setting times of 160 min and 220 min respectively. Fly ash is Grade II fly ash produced by Fenxi Mining Group Power Co. The coal gangue aggregate used is collected from the Xinyang coal mine of Fenxi Mining Group, with an apparent density of 2900 kg/m³ and a crushing size range of 0.1 mm to 20 mm. Water is ordinary tap water. The main chemical composition of the raw materials is shown in Table 1. The chemical composition, microscopic morphology, and particle size distribution of cement and fly ash were obtained by X-ray diffractometer (XRD), scanning electron microscope (SEM), and laser particle size distribution meter (BT-9300HT), respectively, as shown in Fig. 1. The XRD patterns and SEM patterns of coal gangue are shown in Fig. 2.

Table 1 Main chemical compositions of raw material

Chemical composition	Cement/%	Fly ash/%	Coal gangue/%
SiO ₂	22.36	52.42	35.46
Al ₂ O ₃	5.53	32.48	16.11
Fe ₂ O ₃	3.46	3.62	3.86
CaO	65.08	0.99	7.15
MgO	2.1	1.01	3.50
TiO ₂	—	1.26	0.80

Preparation of CGBM specimens

Define the aggregate particle size distribution function as (Chun and Liu 2002):

$$F(\phi) = \frac{N(\phi)}{N_0} \tag{1}$$

where $F(\phi)$ is the aggregate size distribution function; ϕ is the characteristic size of aggregate particles, i.e., particle size, mm; $N(\phi)$ is the total number of aggregates with particle size not larger than ϕ ; N_0 is the total number of aggregates in the aggregate system.

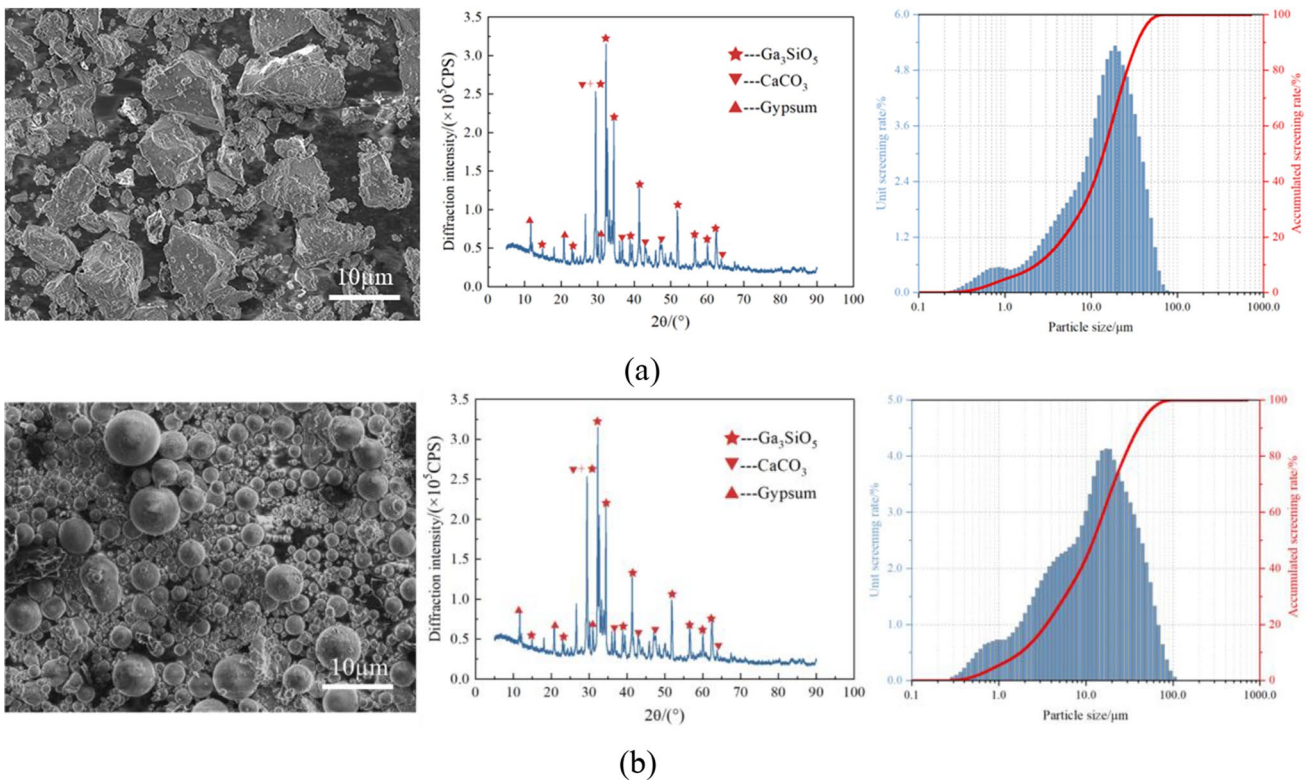
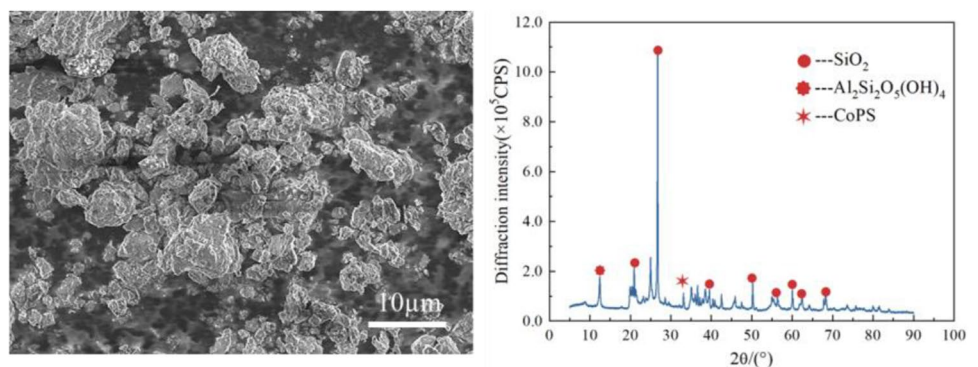


Fig. 1 SEM, XRD, and particle size distribution of cement and fly ash (a) Cement (b) Fly ash

Fig. 2 SEM and XRD of coal gangue



According to Cantor’s fractal theory, it is obtained that

$$N = N_1 \left(\frac{\phi}{\phi_{\max}} \right)^{-D} \tag{2}$$

where N_1 is a constant; ϕ_{\max} is the maximum particle size of the aggregate; D is the fractal dimension of the particle size distribution.

Substituting Eq. (2) into Eq. (1) and applying $F(\phi_{\max}) = 1$, we obtain

$$F(\phi) = \left(\frac{\phi}{\phi_{\max}} \right)^{-D} \tag{3}$$

Similarly, the aggregate mass distribution function is defined as

$$P(\phi) = \frac{M(\phi)}{M_0} \tag{4}$$

where $P(\phi)$ is the aggregate mass distribution function; $M(\phi)$ is the total mass of aggregate with particle size not larger than; M_0 is the total mass of aggregate in the system.

From Eq. (4) we obtained

$$dM(\phi) = M_0 dP(\phi) \tag{5}$$

From the relationship between mass and volume, it follows that

$$dM(\phi) = \rho V(\phi) dN(\phi) \tag{6}$$

where ρ is the aggregate density; $V(\phi)$ is the volume of aggregate in the interval $(\phi, \phi + d\phi)$; $N(\phi)$ is the number of aggregates in the interval $(\phi, \phi + d\phi)$.

From the volume dimension, it follows that

$$V(\phi) = k\phi^3 \tag{7}$$

where k is the volume shape factor of the aggregate.

From Eq. (1), it is obtained that

$$dN(\phi) = N_0 dF(\phi) \tag{8}$$

From Eq. (3), it is obtained that

$$dF(\phi) = -D\phi_{\max}^D \phi^{1-D} d\phi \tag{9}$$

Equations (5), (6), (7), (8), and (9) are combined and integrated to obtain

$$P(\phi) = -\frac{k\rho N\phi_{\max}^D}{M_0(3-D)} \phi^{3-D} + C \tag{10}$$

where, C is the integration constant.

Substituting the boundary conditions $P(\phi_{\max}) = 1$ and $P(\phi_{\min}) = 0$, into Eq. (10) we obtain

$$P(\phi) = \frac{M(\phi)}{M_0} = \frac{\phi^{3-D} - \phi_{\min}^{3-D}}{\phi_{\max}^{3-D} - \phi_{\min}^{3-D}} \tag{11}$$

where, ϕ_{\min} is the minimum particle size of the aggregate, mm.

Since the term ϕ_{\min}^{3-D} for the minimum particle size of the aggregate is extremely small, a simple linearization of Eq. (11) is obtained as

$$\lg \frac{M(\phi)}{M_0} \propto (3 - D) \lg \phi \tag{12}$$

The gangue was sieved into 8 grain levels (<0.15 mm, 0.15 ~ 0.30 mm, 0.30 ~ 0.60 mm, 0.60 ~ 1.18 mm, 1.18 ~ 2.36 mm, 2.36 ~ 5.00 mm, 5.00 ~ 10.00 mm, 10.00 ~ 15.00 mm), and then the distribution of gangue aggregate particle size was regulated based on fractal theory. The distribution mass percentage of gangue aggregate and the fitting results based on Eq. (12) are shown in Figs. 3 and 4. Five groups of aggregates with different particle size distributions were finally obtained, and their fractal dimensions were 2.002, 2.199, 2.401, 2.600, and 2.802, respectively.

The dry ingredients (gangue, cement, and fly ash) were put into the mixer and mixed fully for 4 min, followed by adding mixing water and mixing fully for 4 min. The mixing procedure and time were fixed for all CGBM specimens. The temperature during mixing and testing was always maintained at 20 ± 2 °C.

Test procedure

The slump test method was referred to the standard “Standard for test method of performance on ordinary fresh concrete” (GB/T 50080–2016). The slump cylinder (top diameter 100 mm, bottom diameter 200 mm, height 300 mm) was placed on a flat, smooth, and moistened glass plate beforehand. The mixed mixture was loaded into the conical bucket in layers, ensuring that the loading process was completed within 120 s. The slump cylinder is lifted in a direction perpendicular to the ground within 5 s, and the slump is measured after the CGBM mixture no longer collapses or the slump cylinder is lifted for 30 s.

The rheological parameters were determined by using GERMANN ICAR rheometer. And the experimental procedure and the composition of the rheometer are shown in Fig. 5. The diameter of the rheometer barrel was 286 mm; the stirred CGBM mixture was loaded into the barrel. Then, the paddle blade with a height and diameter of 127 mm was fixed in the center of the barrel so that the distance between the blade and the mixture at the bottom and top of the barrel was 89 mm. Firstly, the static

Fig. 3 Distribution mass percentage of gangue aggregate

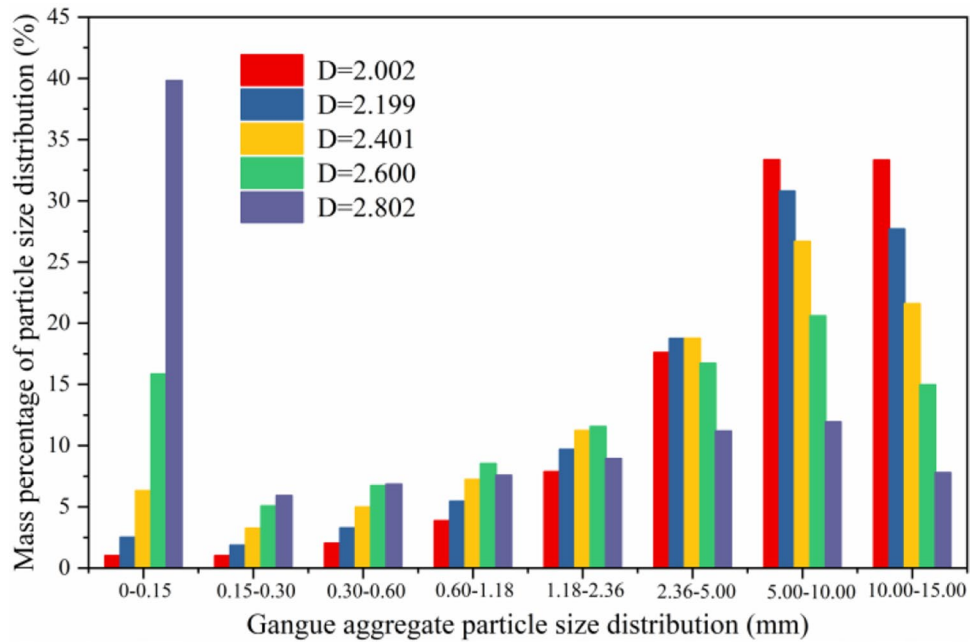
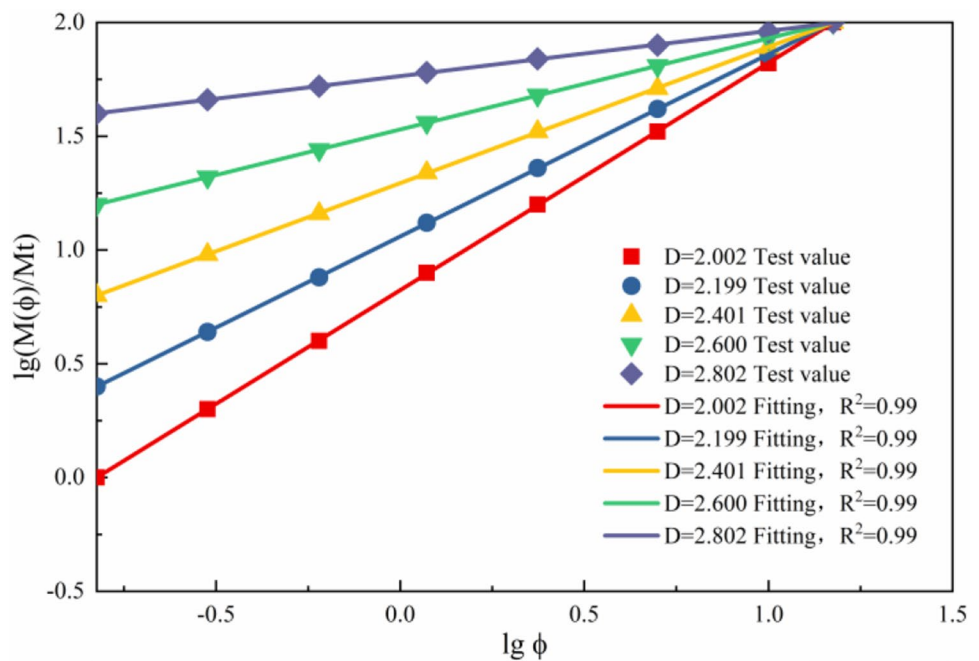


Fig. 4 Fractal dimension of the particle size distribution of gangue aggregate



yield stress was determined by rotating the blade at a constant low rate of 0.025rev/s for 30 s (Rahman et al. 2014). Afterward, the flow curve test was performed to determine the dynamic yield stress and plastic viscosity of the CGBM mixture, and the flow curve test procedure is shown in Fig. 6. The flow curve testing process was divided into two parts: shear failure and reduced speed shear. Pre-testing is preceded by 20 s of rotation at a maximum test speed of 0.5 rev/s, which was designed to

disrupt the flocculation structure of the CGBM mixture to minimize the effect of thixotropy and provide a stable shear history. After shear failure, the rotational speed was equally reduced to 0.05 rev/s and divided into seven test points, each test point lasting 10 s (Baumert and Garrecht 2020; Faraj et al. 2021). The first test time was recorded as 0 min, then every 30 min repeated mixing, slump test, and rheological test and record the rheological parameters of CGBM mixture within 60 min.

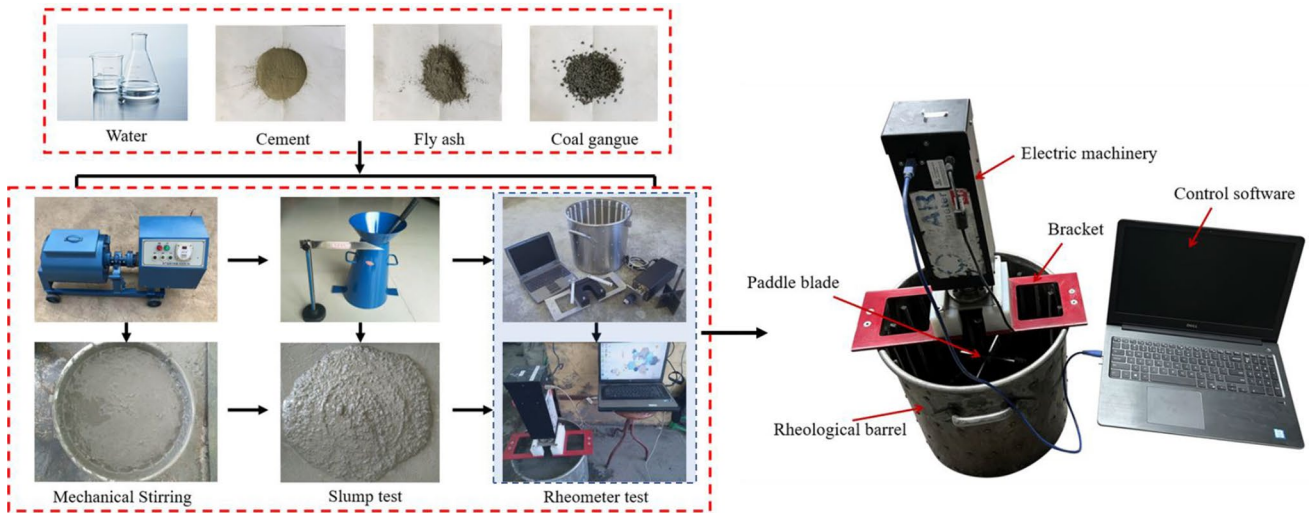
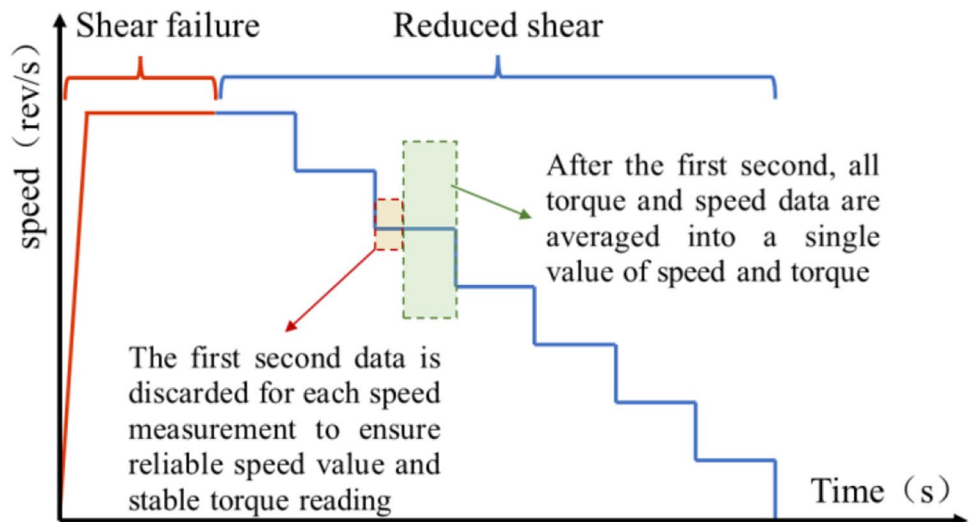


Fig. 5 Experimental flow chart and ICAR rheometer components

Fig. 6 Flow curve test



Results and discussion

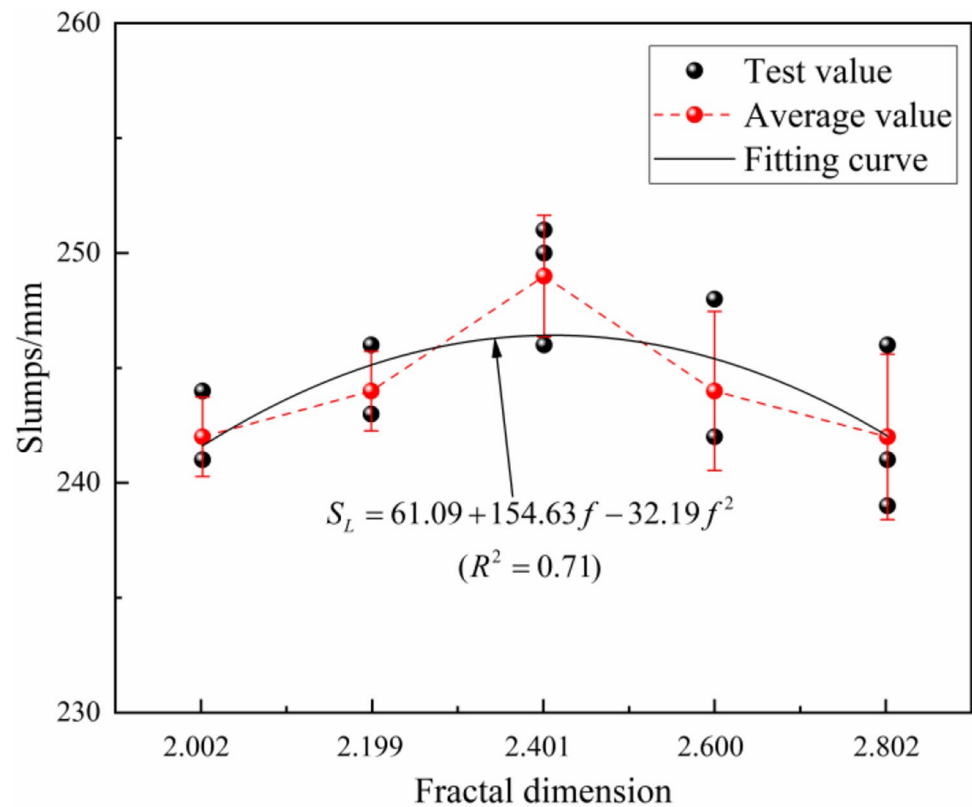
Rheological properties of CGBM

Slump

The influence of gangue aggregate particle size distribution on the slump of CGBM mixture is shown in Fig. 7. The slump of mixture with fractal dimensions of 2.002, 2.199, 2.401, 2.6, and 2.802 are 242 mm, 244 mm, 249 mm, 244 mm, and 242 mm respectively. According to the results, it can be seen that the slump of CGBM mixture rises first with the increment of fractal dimension. In accordance with the theory of excess paste, the voids between the coarse aggregate are filled by fine aggregates,

and the voids between fine aggregates are filled by paste. And the remaining paste is wrapped in the surface of the aggregate to form a lubricating layer, enabling the mixture to flow stably, which is called excess paste (Shi et al. 2018). In the case of a certain paste content in the CGBM mixture, when the fractal dimension of the aggregate particle size distribution increases from 2.002, the increase in the mass fraction of fine aggregates makes the degree of particle accumulation in the aggregate system more compact. The paste filling the voids between the aggregates is reduced; thus, the thickness of the excess paste wrapped around the surface of the aggregate increases, which enlarges the spacing of the aggregate particles. The mechanical engagement force and friction between the aggregates are dropped, and the fluidity of the CGBM is increased, which is manifested by a certain degree of

Fig. 7 Relationship between slump and fractal dimensions



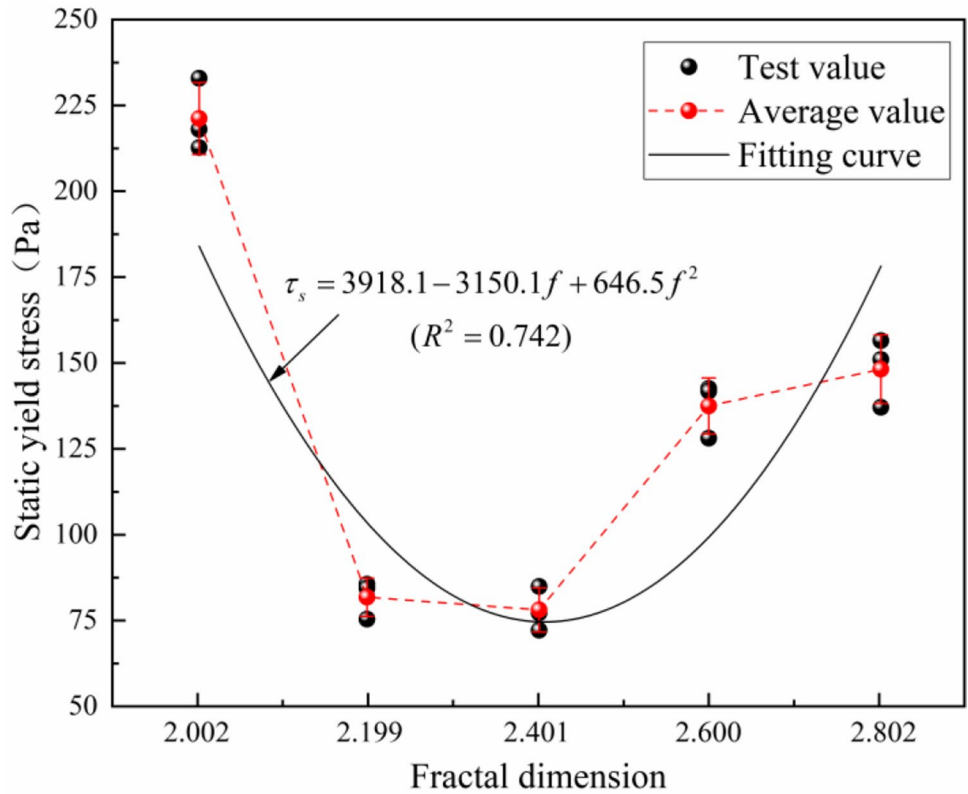
increase in the slump of the CGBM mixture. However, when the fractal dimension exceeds a certain threshold value (between 2.401 and 2.6), the slump starts to decrease with the increase of the fractal dimension. It is evident that when the fine aggregate content increases, the total specific surface area of the aggregate system increases so that the water requirement of the solid particles increases (Cepuritis et al. 2017). Therefore, with the same water consumption, the growth of the total specific surface area increases the paste required to wrap around the surface of the aggregate. This reduces the thickness of the excess paste, resulting in the decrease of the slump of the CGBM mixture.

Static yield stress

In the CGBM mixture two-phase suspension system, the cement paste and the fine gangue aggregate as a homogeneous carrier, and coarse gangue aggregate distributed in this homogeneous carrier uniformly. When the CGBM mixture is at rest, cement particles, hydration products, and fine aggregates lap each other to form a three-dimensional network structure with certain shear strength and wrap with coarse aggregates. Static yield stress is the minimum shear stress that breaks the three-dimensional network structure to make the fluid flow from the resting state (Qian and Kawashima 2016). The impact of the distribution of gangue aggregate

particle size on the static yield stress of CGBM is shown in Fig. 8. The fractal dimensions are 2.002, 2.199, 2.401, 2.6, and 2.802 of the slurry; static yield stress are 221.2 Pa, 84.4 Pa, 78.1 Pa, 137.5 Pa, and 148.2 Pa. It can be seen that the static yield stress of the CGBM with the increase in the fractal dimension of the aggregate presents the trend of decreasing after increasing, and the increase is more slowly. It was attributed to the fact that when the fractal dimension of aggregate particle size distribution increased from 2.002, the mass fraction of fine aggregate also increased gradually as shown in Fig. 3. The density of the homogeneous carrier becomes larger with the increase of fine aggregate, and the floating force of coarse aggregate in the homogeneous carrier increases, which reduces the settling of coarse aggregate to some extent. When most of the coarse aggregate is suspended in the homogeneous carrier, the chance of friction and collision between the coarse aggregate and the bottom and wall of the rheological barrel is reduced, which reduces the resistance during the flow of the slurry. The macroscopic manifestation is the reduction of static yield stress. When the fractal dimension exceeds 2.401, the water flowing between the particles is reduced, due to the larger specific surface area of fine aggregate, which can easily gather with cement particles and their hydration products and form flocs or three-dimensional mesh structure. Therefore, as the fine aggregate continues to increase, the flocculation between fine particles also increases, resulting in the increase of static

Fig. 8 Relationship between static yield stress and fractal dimensions



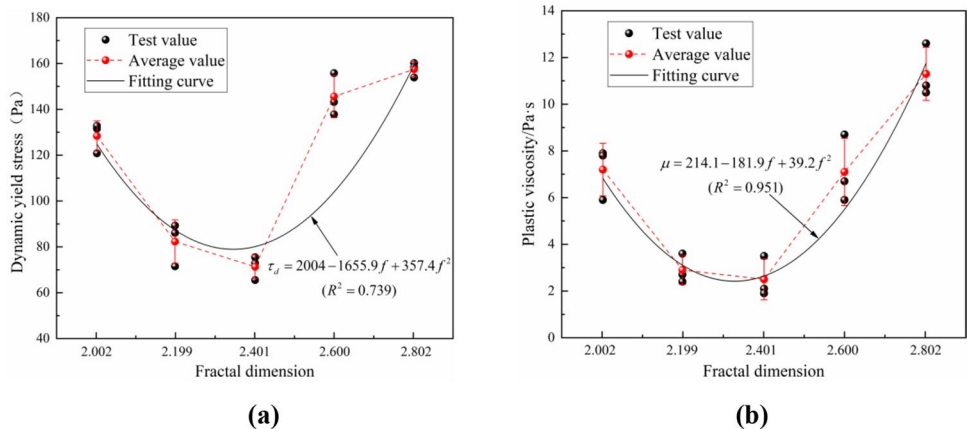
yield stress of the CGBM. The observed effect of adding fine aggregate to increase the static yield stress is consistent with the research of Ivanova and Mechtcherine (2020).

Dynamic yield stress and plastic viscosity

Dynamic yield stress is the minimum stress to maintain the fluid in the flow state, mainly generated by the friction between the particles, reflecting the ease of slurry flow. Plastic viscosity is the rate of deformation of fluid under the action of shear force. It is mainly formed by the interaction force between particles, Brownian motion molecular

force, cement hydration force, and inter-particle viscous force, which can reflect the relationship between the shear stress and shear rate of the fluid, as well as the impeding effect of the internal structure of the fluid on its flow (Li et al. 2017). Figure 9 shows the influence of different gangue aggregate particle size distributions on the dynamic yield stress and plastic viscosity of the CGBM. It can be seen that the dynamic yield stress and plastic viscosity of the CGBM have a similar trend, which decrease first with the increase of the fractal dimension of the aggregate. However, when the fractal dimension exceeds 2.401, the dynamic yield stress and plastic viscosity started to increase gradually. Four

Fig. 9 Relationships between dynamic yield stress, plastic viscosity, and fractal dimensions (a) Dynamic yield stress (b) Plastic viscosity



types of forces exist in the slurry system, which are: colloidal forces, Brownian forces, hydrodynamic forces, and contact forces (Brader 2010). However, colloidal and Brownian forces do not exist between the aggregates because the size of the aggregates is already large enough. When the volume fraction of fine aggregates exceeds a critical value, the hydration forces between the aggregates and the net cement paste dominate. When the volume percentage of fine aggregate exceeds a critical value, the contact forces between the aggregates dominate (Li et al. 2022). Westerholm et al. (2008) investigated the effect of fine aggregate gradation on the rheological properties of mortars and came to similar conclusions. This indicates that the addition of a large number of fine aggregates increases the friction and interaction force between the aggregate particles, which is probably related to the change of the accumulation state between the gangue aggregates.

Time-dependent rheological properties of CGBM

Static yield stress

The time-dependent static yield stress of CGBM within 60 min is shown in Fig. 10. As can be seen, the static yield stress of the CGBM tends to increase significantly with time due to the hydration of the cement and the flocculation between the hydration products and the aggregates. The static yield stresses of the CGBM with fractal dimensions of 2.002, 2.199, 2.401, 2.600, and 2.802 increase by 34.13%, 28.48%, 31.37%, 22.55%, and 31.38% in 30 min, respectively. The static yield stresses in 60 min increase by 28.65%, 31.21%, 23.1%, 21.01%, and 31.07%, respectively. It has been revealed in many research that static yield stress

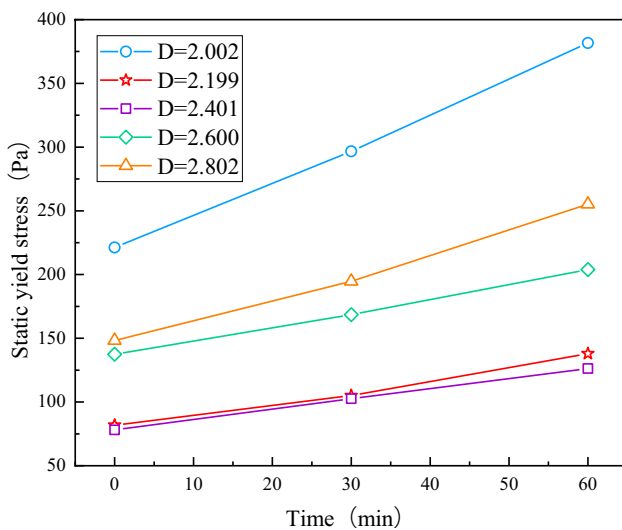


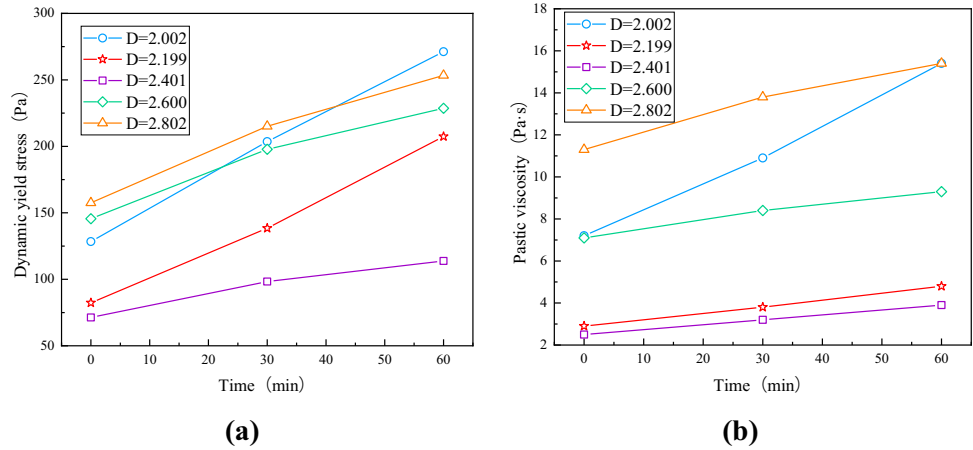
Fig. 10 Variation of static yield stress with time

can characterize the thixotropy of cementitious materials (Williams et al. 1999). Thixotropy is mainly generated by changes in the flocculation structure within the slurry. In the initial stage of cement hydration reaction, when the flocculation structure in the slurry suffers damage, the flocculation structure in the slurry is repaired faster, and the recovery time is short because of the violent hydration reaction. Therefore, the thixotropy is small in this case. With the passage of time, the rate of cement hydration reaction slows down, the recovery time of flocculation structure in the slurry will be greatly extended, and the thixotropy increases. Static yield stress of fractal dimensions of 2.002 and 2.802 is relatively large changes in time. This is due to the fact that when the fine aggregate content is low, there is not enough mortar to wrap the coarse gangue. As a result, the fluidity of the CGBM mixture is poor, and the phenomenon of aggregate segregation and flowing slurry appears with time. When the fine aggregate content is high, the free water in the mortar decreases due to the water absorption of fine aggregate, which further slows down the cement hydration rate and leads to a larger thixotropy of the CGBM. When the fractal dimension is 2.6, the aggregate distribution in the CGBM is optimal, and the transtemporal variation of the static yield stress of the CGBM is small and has good stability.

Dynamic yield stress and plastic viscosity

Figure 11 shows the time-dependent of dynamic yield stress and plastic viscosity of the CGBM for different gangue aggregate particle size distributions within 60 min. Figure 11a shows that the increments of dynamic yield stress in 30 min for slurries with fractal dimensions of 2.002, 2.199, 2.401, 2.600, and 2.802 are 58.57%, 68.17%, 37.87%, 35.85%, and 36.57%, respectively. The increments of dynamic yield stress within 60 min are 33.2%, 49.86%, 15.77%, 15.57%, and 17.81%, respectively. The evolution of the plastic viscosity of the CGBM with different gangue aggregate particle size distribution within 60 min is shown in Fig. 11b. The increments of plastic viscosity in 30 min are 51.39%, 31.03%, 28%, 18.31%, and 22.12% for the slurries with fractal dimensions of 2.002, 2.199, 2.401, 2.600, and 2.802, respectively. And the increments of plastic viscosity in 60 min are 41.28%, 26.32%, 21.88%, 10.71%, and 11.59%, respectively. It can be seen that the dynamic yield stress and plastic viscosity of the CGBM demonstrate a gradual increase with time, which is the result of the interaction between cement hydration and aggregates. This is consistent with the change law of yield stress and plastic viscosity of self-compacting concrete with time studied by Saleh Ahari et al. (2015). On the one hand, the free water in the CGBM gradually decreases with time due to the cement hydration and the water absorption of fine aggregates, which increases the flow resistance of the CGBM. On the other

Fig. 11 Variations of dynamic yield stress and plastic viscosity with time **(a)** Dynamic yield stress **(b)** Plastic viscosity



hand, the friction between the aggregate particles in the CGBM causes the dynamic yield stress and plastic viscosity of the CGBM to become larger. The increase of dynamic yield stress and plastic viscosity of the CGBM is relatively large for the fractal dimensions of 2.002 and 2.199. The reason is that when the fine aggregate is not enough to form a lubricating layer on the gangue surface, which reduces the fluidity of the slurry. While the fine aggregate is excessive, it will also reduce the fluidity of the slurry, and with the growth of time, the phenomenon of aggregate settlement, and segregation. Cheng et al. (2018) performed rheological experiments on paste filling material and combined them with fine-scale image analysis techniques to suggest that the gradation structure forms the basis for the plasticity and stability of the slurry. The flocculent network structure transforms free water into semi-stable forms of adsorbed water and thus causes macroscopic evolution of rheological parameters. The smooth increase in dynamic yield stress and plastic viscosity of the CGBM mixture for fractal dimensions of 2.401 and 2.6 indicates that the slurry at this gradation is more stable and has better water retention and cohesion.

Correlation between rheological parameters and fractal dimension

As shown in Figs. 8 and 9, the yield stress and plastic viscosity decrease first and then increase with the increase of the fractal dimension of the aggregate. To analyze the relationship between the rheology and fractal dimension of the CGBM mixture with different gangue aggregate particle size distribution quantitatively, a quadratic polynomial model was fitted. The fitting results and their correlations are shown in Table 2, where τ_s is the static yield stress, Pa; τ_d is the dynamic yield stress, Pa; μ is the plastic viscosity, Pa s.

According to Table 2, the correlation coefficients of static yield stress and aggregate fractal dimensions of the CGBM mixture are 0.742, 0.787, and 0.839 within 60 min.

Table 2 Correlation between rheological parameters and fractal dimension of aggregate within 60 min

Time	Rheological parameter fitting results	R^2
0 min	$\tau_s = 3918.1 - 3150.1D + 646.5D^2$	0.742
	$\tau_d = 2004 - 1655.9D + 357.4D^2$	0.739
	$\mu = 214.1 - 181.9D + 39.2D^2$	0.951
30 min	$\tau_s = 5445.2 - 4380.1D + 897.4D^2$	0.787
	$\tau_d = 3155.6 - 2563.1D + 542.2D^2$	0.721
	$\mu = 307.6 - 258.3D + 54.9D^2$	0.945
60 min	$\tau_s = 7329.3 - 5907.4D + 1210.5D^2$	0.839
	$\tau_d = 4148.8 - 3314.8D + 688.6D^2$	0.703
	$\mu = 406.7 - 337.6D + 70.75D^2$	0.929

This indicates that the correlation between static yield stress and aggregate fractal dimension increase with time, which reveals that the static yield stress of the CGBM is obviously influenced by the distribution of aggregate particle size with time. The correlation coefficients between the dynamic yield stress and the aggregate fractal dimensions of the CGBM are 0.739, 0.721, and 0.703, and the correlation coefficients between the plastic viscosity force and the aggregate fractal dimensions are 0.951, 0.945, and 0.929, respectively, within 60 min. This demonstrates that the degree of influence of the aggregate size distribution on the dynamic yield stress and plastic viscosity of the CGBM decreases with time. The reason for this is that the hydration products C-S-H generated by the hydration of cement and the fine gangue aggregates lap each other to form a flocculation network structure. With the growth of time, more and more hydration products are generated by hydration, which leads to the formation of a closer flocculation structure around the aggregates and larger flow resistance of the CGBM (Roussel et al. 2012). Consequently, it results in a greater sensitivity of the aggregate particle size distribution to the static yield stress of the

CGBM and less sensitivity to the dynamic yield stress and plastic viscosity.

Mechanistic analysis based on CPM

De. Larrard. F proposed the compressible packing model (CPM) based on the linear packing compactness model and the solid suspension model. The CPM can determine the actual packing density of the mixed aggregate system according to the gradation and proportion of the aggregate in the aggregate system, that is, the percentage of the solid volume in the volume of the whole system when each aggregate in the system is stacked and keeps its original shape. CPM fully takes into account the interaction between particle grades and the effect of different stacking forms on particle packing density by introducing the “loosening effect” and “wall attachment effect.” And CPM is a semi-theoretical and semi-empirical model for predicting the packing density, which is more applicable among many particle packing models applied in the concrete field. Therefore, CPM is used to calculate the aggregate packing density and thus to explain the variation of material rheological properties in this paper. The calculation process of CPM is as follows (Larrard 1999; Chen 2015; Nie 2008; Huang 2021):

Firstly, determine the characteristic particle size d_i as follow:

$$\log_{10}(d_i) = [\log_{10}(d_{\max}) + \log_{10}(d_{\min})]/2 \tag{13}$$

where, d_{\max} and d_{\min} are the maximum particle size and minimum particle size of each particle size range respectively. According to the actual packing compactness α_i of each particle size, compaction index K (taken as 4.75 for the pounded gangue aggregate), and the formula (14), the residual packing compactness β_i of each particle size can be obtained.

$$\alpha_i = \frac{\beta_i}{1 + \frac{1}{K}} \tag{14}$$

Calculate the coefficient of loosening effect coefficient a_{ij} and wall attachment effect coefficient b_{ij} according to formula (15) and formula (16).

$$a_{ij} = \sqrt{1 - (1 - d_j/d_i)^{1.02}} \tag{15}$$

$$b_{ij} = 1 - (1 - d_j/d_i)^{1.50} \tag{16}$$

where, a_{ij} is the loosening effect coefficient of the j grade aggregate on the i grade aggregate; b_{ij} is the wall effect coefficient of the j grade aggregate on the i grade aggregate. And calculate the virtual packing compactness of each particle size according to the following formula:

$$\gamma_i = \beta_i / \left\{ 1 - \sum_{j=1}^{i-1} [1 - \beta_i + b_{ij}\beta_i(1 - 1/\beta_i)]y_j - \sum_{j=i+1}^n [1 - a_{ij}\beta_i/\beta_j]y_j \right\} \tag{17}$$

Calculate the actual packing compactness γ_i of the mixture according to the following formula (18); y_j is the volume fraction of the j grade aggregate; Φ is the actual packing compactness of the mixed aggregate system.

$$K = \sum_{i=1}^n K_i = \sum_{i=1}^n \frac{y_i/\beta_i}{1/\Phi - 1/\gamma_i} \tag{18}$$

Set the function $H(\Phi)$ as follows:

$$H(\Phi) = \sum_{i=1}^n \frac{y_i/\beta_i}{1/\Phi - 1/\gamma_i} - K \tag{19}$$

Solve for the minimum of Φ in the interval (0,1). This value is the actual packing compactness of the mixed aggregate system.

The calculation results of the actual stacking compactness of gangue aggregate system with different fractal dimensions are shown in Table 3.

As can be seen from Table 3, the packing compactness of gangue aggregate system increases first and then decreases with the increase of fractal dimension. When the fractal dimension is less than 2.6, coarse aggregate pile is dominant, and the “loosening effect” between the aggregate particles dominates. Since the fine gangue is filled in the “skeleton” structure system composed of coarse gangue, the degree of embedding between the gangue aggregates gradually increased, which leads to the accumulation of aggregate system dense degree is increasing. In the case of the same cement paste volume, the thickness of the excess paste in the slurry keeps increasing, so that the distance between the gangue aggregates keeps increasing. While reducing the frictional collision between the aggregates, the free water channels in the slurry are continuously developed, and the pore water is released, which improves the fluidity of the CGBM, and the macroscopic manifestation is the corresponding reduction of yield stress and plastic viscosity. When the fractal dimension of the aggregate is 2.6, the actual packing density of the aggregate system reaches the maximum value of 0.746, the fitting degree between the gangue aggregates reaches the maximum, the excess paste also reaches the maximum thickness, and the pore water in the CGBM is fully released, at which time the CGBM has the best flowability and the yield stress and plastic viscosity reach the minimum value. When the fractal dimension exceeds 2.6, fine

Table 3 Calculation results of actual stacking compactness

Fractal dimension D	2.002	2.199	2.401	2.600	2.802
Actual packing compactness Φ	0.739	0.695	0.726	0.746	0.678

gangue in the gangue aggregate system has been excessive. Fine gangue dominates, and coarse gangue randomly dispersed in the fine gangue group, which result the closest fitting state of the aggregate system destroyed. In this case, the packing compactness of the aggregate system is mainly affected by the “wall attachment effect.” Therefore, the packing density of the aggregate system decreases with the increase of fractal dimension. In this process, the thickness of the excess paste in the CGBM begins to decrease, the probability of friction and collision between the aggregates increases, and the free water channel also decreases. The pore water is wrapped by the mutually embedded gangue aggregate, and the CGBM loses part of its fluidity, resulting in a corresponding increase in yield stress and plastic viscosity.

Conclusion

In this study, the influence of aggregate with different particle size distribution on rheological properties of CGBM mixture was investigated, and the relationships between fractal dimensions and rheological parameters were established. According to the results obtained, the following conclusions can be drawn:

- (1) The static yield stress, dynamic yield stress, and plastic viscosity of CGBM are decreasing with the increase of aggregate fractal dimension and then increasing trend. When the aggregate fractal dimension is in the range of 2.401 ~ 2.6, the flowability of the CGBM is better.
- (2) The static yield stress, dynamic yield stress, and plastic viscosity increase with the passage of time, and the increase rate gradually decreases. The rheological parameters of CGBM with aggregate fractal dimensions of 2.401 and 2.6 have little influence on time, and the CGBM stability is better.
- (3) The relationship between fractal dimension and rheological parameters can be fitted by quadratic polynomial. The static yield stress is influenced by the distribution of aggregate size gradually becomes larger with time, and the dynamic yield stress and plastic viscosity are influenced by the distribution of aggregate size gradually decreases with time.
- (4) With the increase of fractal dimension, the packing density of gangue aggregate increases first and then decreases. When the fractal dimension of the aggregate is 2.6, the stacking compactness of the gangue aggregate system reaches the maximum, and the pore water in the CGBM is fully released. In this case, the yield stress and plastic viscosity of the CGBM are the lowest, which indicates that the reasonable particle

size distribution of the aggregate can improve the flow performance of the CGBM.

It is necessary to further study the rheological properties of CGBM in pipelines. Before the full application of CGBM, the mechanical properties of gangue cemented filling materials should also be studied.

Author contribution XY: experiment, data collection, and drafting. YG: funding acquisition, methodology, and supervising all stages of manuscript preparation. GF: investigation, financing, and supervision. XW, WH, and JM: supervision, review, editing, and conceptualization. All authors have read, revised, approved, and agreed to the contents of the final version of this review.

Funding This study was sponsored by the National Natural Science Foundation of China (Grant No. 51974192), the Distinguished Youth Funds of National Natural Science Foundation of China (Grant No. 51925402), and Shanxi-Zheda Institute of Advanced Materials and Chemical Engineering Project (2021SX-TD001).

Data availability The datasets used and/or analyzed during the current study are available from the corresponding author on reasonable request.

Declarations

Ethics approval Not applicable.

Consent to participate Not applicable.

Consent for publication Not applicable.

Competing interests The authors declare no competing interests.

References

- Baumert C, Garrecht H (2020) Minimization of the influence of shear-induced particle migration in determining the rheological characteristics of self-compacting mortars and concretes. *Materials* 13(7):1–11. <https://doi.org/10.3390/ma13071542>
- Brader J (2010) Nonlinear rheology of colloidal dispersions. *J Phys: Condens Matter* 22(36):363101. <https://doi.org/10.1088/0953-8984/22/36/363101>
- Cepuritis R, Jacobsen S, Smeplass S, Mørtzell E, Wigum BJ, Ng S (2017) Influence of crushed aggregate fines with micro-proportioned particle size distributions on rheology of cement paste. *Cem Concr Compos* 80:64–79. <https://doi.org/10.1016/j.cemconcomp.2017.02.012>
- Chen J (2015) Compressible packing model based study of green concrete. Dissertation, Shenzhen University
- Chen M, Wang Y, Tao Y, Wang H (2022a) Impact compression properties of recycled tyre steel fiber reinforced concrete based on fractal theory. *Journal of Northeastern University (Natural Science)* 43(02):266–273. <https://doi.org/10.12068/j.issn.1005-3026.2022.02.016>. (In Chinese)
- Chen Q, Zhou L, Wang Y, Li X, Zhang Q, Feng Y, Qi C (2022b) Resistance loss in cemented paste backfill pipelines: effect of inlet velocity, particle mass concentration, and particle size. *Materials* 15(9):3339. <https://doi.org/10.3390/ma15093339>

- Cheng H, Wu S, Wu A, Cheng W (2018) Grading characterization and yield stress prediction based on paste stability coefficient. *Chin J Eng* 40(10):1168–1176. <https://doi.org/10.13374/j.issn2095-9389.2018.10.003>. (In Chinese)
- Chun X, Liu H (2002) Research on fractal characteristic of the size-distribution of concrete aggregates. *Journal of Southwest Jiaotong University* 37(02):186–189. <https://doi.org/10.3969/j.issn.0258-2724.2002.02.018>. (In Chinese)
- Deng DQ, Liu L, Yao ZL, Song KILL, Lao DZ (2017) A practice of ultra-fine tailings disposal as filling material in a gold mine. *J Environ Manage* 196:100–109. <https://doi.org/10.1016/j.jenvman.2017.02.056>
- Du X, Feng G, Zhang Y, Wang Z, Guo Y, Qi T (2019) Bearing mechanism and stability monitoring of cemented gangue-fly ash backfill column with stirrups in partial backfill engineering. *Eng Struct* 188:603–612. <https://doi.org/10.1016/j.engstruct.2019.03.061>
- Faraj RH, Sherwani AFH, Jafer LH, Ibrahim DF (2021) Rheological behavior and fresh properties of self-compacting high strength concrete containing recycled PP particles with fly ash and silica fume blended. *J Build Eng* 34:101667. <https://doi.org/10.1016/j.jobbe.2020.101667>
- Feng G, Jia X, Guo Y, Qi T, Li Z, Li J, Liu G, Song K (2016) Study on mixture ratio of gangue-waste concrete cemented paste backfill. *J Mining Saf Eng* 33(06):1072–1079. <https://doi.org/10.13545/j.cnki.jmse.2016.06.017>. (In Chinese)
- Feng G, Ran H, Guo J, Guo Y, Li C (2022) Experimental investigation on the deformation and strength properties of cemented gangue backfill column under long-term axial compression. *Structures* 43:1558–1572. <https://doi.org/10.1016/j.istruc.2022.07.068>
- Gao Y, Jing H, Yu Z, Li L, Wu J, Chen W (2022) Particle size distribution of aggregate effects on the reinforcing roles of carbon nanotubes in enhancing concrete ITZ. *Constr Build Mater* 327:126964. <https://doi.org/10.1016/j.conbuildmat.2022.126964>
- Gismera S, Alonso MDM, Palacios M, Puertas F (2020) Rheology of alkali-activated mortars: influence of particle size and nature of aggregates. *Minerals-Basel* 10(8):726. <https://doi.org/10.3390/min10080726>
- Guo Y, Wang P, Feng G, Qi T, Du X, Wang Z, Li Q (2020) Experimental study on diffusion process of sulfate ion in cemented gangue backfill material. *Adv Civ Eng* 2020:1–14. <https://doi.org/10.1155/2020/5846397>
- Guo Y, Ran H, Feng G, Du X, Zhao Y, Xie W (2022) Deformation and instability properties of cemented gangue backfill column under step-by-step load in constructional backfill mining. *Environ Sci Pollut Res* 29(2):2325–2341. <https://doi.org/10.1007/s11356-021-15638-z>
- Hu J, Wang K (2011) Effect of coarse aggregate characteristics on concrete rheology. *Constr Build Mater* 25(3):1196–1204. <https://doi.org/10.1016/j.conbuildmat.2010.09.035>
- Huang Y (2021) Study on rheological properties of manufactured sand mortar based on compact packing. Dissertation, Guangzhou University
- Ivanova I, Mechtcherine V (2020) Effects of volume fraction and surface area of aggregates on the static yield stress and structural build-up of fresh concrete. *Materials* 13(7):1551. <https://doi.org/10.3390/ma13071551>
- Larrard F (1999) Concrete mixture proportioning: a scientific approach. Routledge, New York
- Li H, Huang F, Cheng G, Yi Z, Zhang Y, Zhang Z, Xie Y (2017) Effect of water-power ratio on shear deformation behavior of self-compacting concrete (SCC). *J Build Mater* 20(01):30–35. <https://doi.org/10.3969/j.issn.1007-9629.2017.01.006>. (In Chinese)
- Li Y, Zhai Y, Liu X, Liang W (2019) Research on fractal characteristics and energy dissipation of concrete suffered freeze-thaw cycle action and impact loading. *Materials* 12(16):2585. <https://doi.org/10.3390/ma12162585>
- Li B, Hou S, Duan Z, Li L, Guo W (2021) Rheological behavior and compressive strength of concrete made with recycled fine aggregate of different size range. *Constr Build Mater* 268:121172. <https://doi.org/10.1016/j.conbuildmat.2020.121172>
- Li T, Zhou Y, Zhu J, Liu J (2022) Effect of fine aggregate gradation on the rheology of mortar. *Constr Build Mater* 332:127362. <https://doi.org/10.1016/j.conbuildmat.2022.127362>
- Liang W, Zhao J, Li Y, Zhai Y (2020) Research on the fractal characteristics and energy dissipation of basalt fiber reinforced concrete after exposure to elevated temperatures under impact loading. *Materials* 13(8):1902. <https://doi.org/10.3390/ma13081902>
- Liu X, Su X, Huang X, Tan W (2016) Study on pipeline transport drag reduction technology of CPB based on the fuller grading theory. *Metal Mine* 10:40–44. <https://doi.org/10.3969/j.issn.1001-1250.2016.10.009>. (In Chinese)
- Mahaut F, Mokéddem S, Chateau X, Roussel N, Ovarlez G (2008) Effect of coarse particle volume fraction on the yield stress and thixotropy of cementitious materials. *Cement Concrete Res* 38(11):1276–1285. <https://doi.org/10.1016/j.cemconres.2008.06.001>
- Nie J (2008) Study on performance of cement-based composite materials based on compressible packing model. Dissertation, Hunan University
- Qi T, Feng G, Li Y, Guo Y, Guo J, Zhang Y (2015) Effects of fine gangue on strength, resistivity, and microscopic properties of cemented coal gangue backfill for coal mining. *Shock Vib* 2015:1–11. <https://doi.org/10.1155/2015/752678>
- Qian Y, Kawashima S (2016) Use of creep recovery protocol to measure static yield stress and structural rebuilding of fresh cement pastes. *Cem Concr Res* 90:73–79. <https://doi.org/10.1016/j.cemconres.2016.09.005>
- Rahman MK, Baluch MH, Malik MA (2014) Thixotropic behavior of self compacting concrete with different mineral admixtures. *Constr Build Mater* 50:710–717. <https://doi.org/10.1016/j.conbuildmat.2013.10.025>
- Ran H, Guo Y, Feng G, Li C (2022) Failure properties and stability monitoring of strip and column cemented gangue backfill bodies under uniaxial compression in constructional backfill mining. *Environ Sci Pollut Res* 29(34):51411–51426. <https://doi.org/10.1007/s11356-022-19336-2>
- Ren W, Xu J (2016) Fractal characteristics of concrete fragmentation under impact loading. *J Mater Civ Eng* 29(4):04016244. [https://doi.org/10.1061/\(ASCE\)MT.1943-5533.0001764](https://doi.org/10.1061/(ASCE)MT.1943-5533.0001764)
- Roussel N, Ovarlez G, Garrault S, Brumaud C (2012) The origins of thixotropy of fresh cement pastes. *Cem Concr Res* 42(1):148–157. <https://doi.org/10.1016/j.cemconres.2011.09.004>
- Saleh Ahari R, Erdem TK, Ramyar K (2015) Time-dependent rheological characteristics of self-consolidating concrete containing various mineral admixtures. *Constr Build Mater* 88:134–142. <https://doi.org/10.1016/j.conbuildmat.2015.04.015>
- Shi C, Wang D, An X, Jiao D, Li H (2018) Method for mixture design of concrete with multiple performance requirements. *J Chin Ceram Soc* 46(02):230–238. <https://doi.org/10.14062/j.issn.0454-5648.2018.02.09>. (In Chinese)
- Sun Q, Tian S, Sun Q, Li B, Cai C, Xia Y, Mu Q (2019) Preparation and microstructure of fly ash geopolymer paste backfill material. *J Clean Prod* 225:376–390. <https://doi.org/10.1016/j.jclepro.2019.03.310>
- Wang Z, Feng G, Qi T, Guo Y, Du X (2020) Evaluation of static segregation of cemented gangue-fly ash backfill material using electrical resistivity method. *Measurement* 154:107483. <https://doi.org/10.1016/j.measurement.2020.107483>
- Wang A, Cao S, Yilmaz E (2022) Effect of height to diameter ratio on dynamic characteristics of cemented tailings backfills with fiber reinforcement through impact loading. *Constr Build Mater* 322:126448. <https://doi.org/10.1016/j.conbuildmat.2022.126448>

- Westerholm M, Lagerblad B, Silfwerbrand J, Forssberg E (2008) Influence of fine aggregate characteristics on the rheological properties of mortars. *Cem Concr Compos* 30(4):274–282. <https://doi.org/10.1016/j.cemconcomp.2007.08.008>
- Williams DA, Saak AW, Jennings HM (1999) The influence of mixing on the rheology of fresh cement paste. *Cem Concr Res* 29(9):1491–1496. [https://doi.org/10.1016/S0008-8846\(99\)00124-6](https://doi.org/10.1016/S0008-8846(99)00124-6)
- Wu D, Yang B, Liu Y (2015) Pressure drop in loop pipe flow of fresh cemented coal gangue–fly ash slurry: experiment and simulation. *Adv Powder Technol* 26(3):920–927. <https://doi.org/10.1016/j.apt.2015.03.009>
- Wu J, Yin Q, Gao Y, Meng B, Jing H (2021a) Particle size distribution of aggregates effects on mesoscopic structural evolution of cemented waste rock backfill. *Environ Sci Pollut Res* 28(13):16589–16601. <https://doi.org/10.1007/s11356-020-11779-9>
- Wu J, Jing H, Pu H, Zhang X, Meng Q, Yin Q (2021b) Macroscopic and mesoscopic mechanical properties of cemented waste rock backfill using fractal gangue. *Chin J Rock Mech Eng* 40(10):2083–2100. <https://doi.org/10.13722/j.cnki.jrme.2021.0234>. (In Chinese)
- Xue G, Yilmaz E, Feng G, Cao S, Sun L (2021) Reinforcement effect of polypropylene fiber on dynamic properties of cemented tailings backfill under SHPB impact loading. *Constr Build Mater* 279:122417. <https://doi.org/10.1016/j.conbuildmat.2021.122417>
- Yan W, Cui W, Qi L (2020) Effect of aggregate gradation and mortar rheology on static segregation of self-compacting concrete. *Constr Build Mater* 259:119816. <https://doi.org/10.1016/j.conbuildmat.2020.119816>
- Yilmaz E, Belem T, Benzaazoua M (2014) Effects of curing and stress conditions on hydromechanical, geotechnical and geochemical properties of cemented paste backfill. *Eng Geol* 168:23–37. <https://doi.org/10.1016/j.enggeo.2013.10.024>
- Zhao Y, Guo Y, Feng G, Li C, Xie W, Zhang C (2022a) Study on strength and deformation characteristics of cemented gangue backfill body under the coupling action of load and salt erosion. *Constr Build Mater* 342:128003. <https://doi.org/10.1016/j.conbuildmat.2022.128003>
- Zhao Z, Cao S, Yilmaz E (2022b) Effect of layer thickness on the flexural property and microstructure of 3D-printed rhomboid polymer-reinforced cemented tailing composites. *Int J Miner, Metal Mater*. <https://doi.org/10.1007/s12613-022-2557-6>
- Zhang Q, Hu G, Wang X (2008) Hydraulic calculation of gravity transportation pipeline system for backfill slurry. *J Cent South Univ Technol*. <https://doi.org/10.1007/s11771-008-0120-x>

Publisher's note Springer Nature remains neutral with regard to jurisdictional claims in published maps and institutional affiliations.

Springer Nature or its licensor (e.g. a society or other partner) holds exclusive rights to this article under a publishing agreement with the author(s) or other rightsholder(s); author self-archiving of the accepted manuscript version of this article is solely governed by the terms of such publishing agreement and applicable law.